

# Unbiased Monte Carlo Cluster Updates with Autoregressive Neural Networks

Dian Wu,<sup>\*</sup> Riccardo Rossi,<sup>†</sup> and Giuseppe Carleo<sup>‡</sup>

*Institute of Physics, École Polytechnique Fédérale de Lausanne (EPFL), CH-1015 Lausanne, Switzerland*

(Dated: December 1, 2021)

Efficient sampling of complex high-dimensional probability densities is a central task in computational science. Machine Learning techniques based on autoregressive neural networks have been recently shown to provide good approximations of probability distributions of interest in physics. In this work, we propose a systematic way to remove the intrinsic bias associated with these variational approximations, combining it with Markov-chain Monte Carlo in an automatic scheme to efficiently generate cluster updates, which is particularly useful for models for which no efficient cluster update scheme is known. Our approach is based on symmetry-enforced cluster updates building on the neural-network representation of conditional probabilities. We demonstrate that such finite-cluster updates are crucial to circumvent ergodicity problems associated with global neural updates. We test our method for first- and second-order phase transitions in classical spin systems, proving in particular its viability for critical systems, or in the presence of metastable states.

Markov-chain Monte Carlo [1] (MCMC) is an unbiased numerical method that allows to sample from unnormalized probability distributions, a central task in many areas of computational science. MCMC is commonly used, for example, in molecular dynamics [2], as well as statistical and quantum physics [3–6]. In addition to fundamental applications, MCMC serves as a physics-inspired approach to solve a variety of computational problems, including combinatorial optimization problems [7, 8], and computer graphics [9]. While MCMC is a generically applicable technique, its implementation can be plagued by long mixing or autocorrelation time [10]. Various techniques have been proposed to increase the efficiency of MCMC [11], e.g. cluster updates [12, 13], parallel tempering [14], the worm algorithm [15], and event-chain Monte Carlo [16]. However, these faster MCMC algorithms rely on details of the model considered, and they cannot be applied generically.

Machine Learning (ML) methods, given their intrinsic flexibility in addressing problems in computational physics [17], are being intensively investigated as a way to improve MCMC. Applications in this direction include, for example, self-learning Monte Carlo methods [18–23], enhanced sampling driven by neural networks [24, 25], neural importance sampling [26], and many more. Strongly rooted in statistical physics principles, variational sampling techniques are among the most promising ML-driven approaches. Generative neural samplers (GNSs) [27–29] are a chief example of ML-driven variational methods. These approaches build on the idea of constructing approximate representations of the original probability distribution at hand. The resulting variational approximations are such that, by construction, sampling can be efficiently performed, thus completely bypassing MCMC. A particularly interesting aspect of this approach is its systematic improvability when using as guiding principle the free energy bound minimization to gauge the approximation accuracy. The main drawback of the variational approach however is

that estimators of expectation values, for example of physical quantities, are intrinsically biased by the representation error of the model distribution. Unbiased estimators are however of central importance in many fundamental applications in physics, thus recent research has started addressing the key problem of removing the bias induced by ML variational representations, for example through importance sampling strategies [26, 30].

In this Letter, we propose a systematic way to efficiently combine variational techniques with MCMC by using autoregressive neural networks [31, 32] as Monte Carlo cluster update proposers. We first show that unbiased schemes using global updates proposed by GNSs can be plagued by ergodicity issues. These arise due to the generic presence of “exponentially suppressed” configurations, which have limited effect on the value of the variational free energy. Our solution to this problem consists of two ingredients. On one hand, we consider symmetry operations that leave the problem Hamiltonian invariant. When applied to states of the neural-enhanced MCMC, these symmetry operations significantly reduce the exponential suppression of configurations belonging to the same equivalence class. On the other hand, we take advantage of autoregressive structure of the neural network representation to propose MCMC updates of clusters of configurations. The resulting cluster proposal is completely automatic, and is therefore particularly helpful for models for which no cluster updates techniques are known. We benchmark our technique in the two-dimensional Ising model, showing that our solution eliminates the ergodicity issues of the global update approach in the critical region. We then study a Ising plaquette model for which traditional cluster algorithms are not applicable, and we find a first-order transition from a paramagnetic state to a “ferrimagnetic” state that breaks a  $\mathbb{Z}_2 \times \mathbb{Z}_2 \times \mathbb{Z}_2$  symmetry of the Hamiltonian. In particular, we show that the method is not affected by metastability issues as it is able to rapidly thermalize by using cluster updates.

*Bias in neural sampling.* In the following we consider a system of  $V$  Ising spins  $\mathbf{s} := (s_1, \dots, s_V)$ ,  $s_i \in \{-1, 1\}$ , at inverse temperature  $\beta$ . We use a GNS  $q_\theta$  with parameters  $\theta$  that variationally approximates the Boltzmann probability distribution  $p(\mathbf{s}) \propto \tilde{p}(\mathbf{s}) := e^{-\beta E(\mathbf{s})}$  by minimizing, in statistical physics language, a free energy bound [27], which is equivalent to minimizing the Kullback–Leibler (KL) divergence [33]

$$D_{\text{KL}}(q_\theta \| p) := \sum_{\mathbf{s}} q_\theta(\mathbf{s}) \ln \frac{q_\theta(\mathbf{s})}{p(\mathbf{s})}. \quad (1)$$

To construct an expressive  $q_\theta$ , we use an autoregressive neural network to decompose it into a product of conditional probabilities  $q_\theta(\mathbf{s}) =: \prod_{i=1}^V q_{\theta;i}(s_i | \mathbf{s}_{<i})$ , where  $\mathbf{s}_{<i} := (s_1, \dots, s_{i-1})$ . This specific choice for the model allows to efficiently sample from the distribution  $q_\theta(\mathbf{s})$  by sampling from the conditional probabilities  $q_{\theta;i}$  sequentially [27].

The autoregressive variational approach is systematically improvable and allows exact sampling. However, the fact that the two distributions are only approximately equal,  $q_\theta(\mathbf{s}) \simeq \tilde{p}(\mathbf{s})$ , also implies that samples  $(\mathbf{s}^{(1)}, \dots, \mathbf{s}^{(N)})$  drawn from the network carry an intrinsic bias. When these samples are used to compute expectation values of some observable, as  $\bar{O} \approx \frac{1}{N} \sum_{i=1}^N O(\mathbf{s}^{(i)})$ , the resulting estimator is biased, and, most importantly, it is not possible in general to reliably estimate the magnitude of such variational bias.

*Neural importance sampling and global updates.* Ref. [30] has proposed two strictly-related solutions to the bias problem. The first method, which we denote neural importance sampling (NIS) in the following, consists in using the modified unbiased estimator  $\bar{O} \approx \sum_{i=1}^N w(\mathbf{s}^{(i)}) O(\mathbf{s}^{(i)})$ , where  $w(\mathbf{s}^{(i)}) := \frac{\tilde{w}(\mathbf{s}^{(i)})}{\sum_{j=1}^N \tilde{w}(\mathbf{s}^{(j)})}$  and  $\tilde{w}(\mathbf{s}^{(i)}) := \frac{\tilde{p}(\mathbf{s}^{(i)})}{q_\theta(\mathbf{s}^{(i)})}$  are the normalized and the unnormalized weights respectively. The second proposed solution, which we denote neural global update (NGU) hereafter, consists in using the GNS as a MCMC proposer: if  $\mathbf{s}$  is the Markov-chain state, a proposed state  $\mathbf{s}'$  is drawn from the GNS and accepted with probability

$$P_{\text{acc}}(\mathbf{s} \rightarrow \mathbf{s}') := \min \left( 1, \frac{\tilde{w}(\mathbf{s}')}{\tilde{w}(\mathbf{s})} \right). \quad (2)$$

*Exponentially suppressed configurations and essential non-ergodicity.* We point out an elementary property of the KL divergence, Eq. (1): the cost of allowing a single bad approximation scales only logarithmically with the ratio of  $p$  and  $q_\theta$ . Therefore, it is reasonable to generically expect that, even when the free-energy is well approximated, for a small number of configurations,  $q_\theta$  is exponentially smaller than the true probability distribution  $p$ . We call them exponentially suppressed configurations (ESCs) [34].

Let us consider a NGU-based Markov chain evolution. Let us suppose that the Markov chain state  $\mathbf{s}$  is an ESC.

The ratio  $\tilde{w}(\mathbf{s}')/\tilde{w}(\mathbf{s})$  in Eq. (2) will be exponentially small for almost any other configuration  $\mathbf{s}'$ , therefore the Markov chain will be essentially stuck in  $\mathbf{s}$  for a long time before accepting any new proposal, and the autocorrelation time of the whole chain will be impractically large. A similar argument applies when considering the variance of the NIS method.

*Symmetry-enforcing cluster updates.* In order to solve the generic ergodicity problem of neural global update methods, we propose a natural method based on the symmetries of the physical system and the chain-like graphical structure of the autoregressive model, which allows to escape from ESCs by symmetry operations and smooth modifications of the configuration.

We start by describing the symmetry-enforcing update. Assuming that the energy of our system is invariant under the action of a symmetry group  $G$  on a given configuration, usually a translation and/or a reflection, at each Monte Carlo step we apply a random element of  $G$  to the configuration [35]. Assuming that the Markov-chain state is an ESC, the probability that all the configurations in an equivalence class of  $G$  are ESCs is very small, and therefore we are able to quickly escape from ESCs. In the following we refer to this method as neural global update with symmetries (NGUS).

With autoregressive neural networks, it is particularly natural to consider cluster updates where only a subset of the lattice is changed. Indeed, for any given  $k$ , it is possible to propose an update  $\mathbf{s} \rightarrow \mathbf{s}'$  by setting  $\mathbf{s}'_{\leq V-k} := \mathbf{s}_{\leq V-k}$  and only sample  $\mathbf{s}'_{> V-k}$ . The weight ratio in Eq. (2) becomes  $\frac{\tilde{w}(\mathbf{s}')}{\tilde{w}(\mathbf{s})} = \frac{\tilde{p}(\mathbf{s}')}{\tilde{p}(\mathbf{s})} \prod_{i=V-k+1}^V \frac{q_{\theta;i}(s_i | \mathbf{s}_{<i})}{q_{\theta;i}(s'_i | \mathbf{s}'_{<i})}$ , which tends towards 1 as  $k \rightarrow 0$ . In this way, the new configuration is closer to the old one and is easier to be accepted, so we expect lower autocorrelation time than global update methods.

As symmetry-enforcing and cluster updates are compatible with each other, we use the two at the same time and we call the resulting method neural cluster updates with symmetries (NCUS), see Alg. 1 and Fig. 1 for a schematic definition and illustration respectively. Although the number of sampled spins  $k$  can be proposed with any distribution  $P_{\text{cluster}}(k)$ , we find that the uniform distribution  $P_{\text{cluster}}(k) \equiv 1/V$  already works well in all the cases we have explored, and accordingly we have not tried to find the optimal choice for it [36].

---

#### Algorithm 1 A step of NCUS.

---

- 1: Input the current configuration  $\mathbf{s}$
  - 2: Sample an integer  $k \in \{1, \dots, V\}$  from  $P_{\text{cluster}}$
  - 3: Sample the last  $k$  spins and propose the configuration  $\mathbf{s}'$
  - 4: Accept  $\mathbf{s} \leftarrow \mathbf{s}'$  with probability  $P_{\text{acc}}(\mathbf{s} \rightarrow \mathbf{s}')$
  - 5: Translate  $\mathbf{s}$  by a random displacement
  - 6: Reflect  $\mathbf{s}$  along  $x$ -axis,  $y$ -axis and the diagonal, each with 50% probability
  - 7: Reflect  $\mathbf{s}$  along  $z$ -axis (flip all spins) with 50% probability
  - 8: Output  $\mathbf{s}$  as a sample in the Markov chain
-

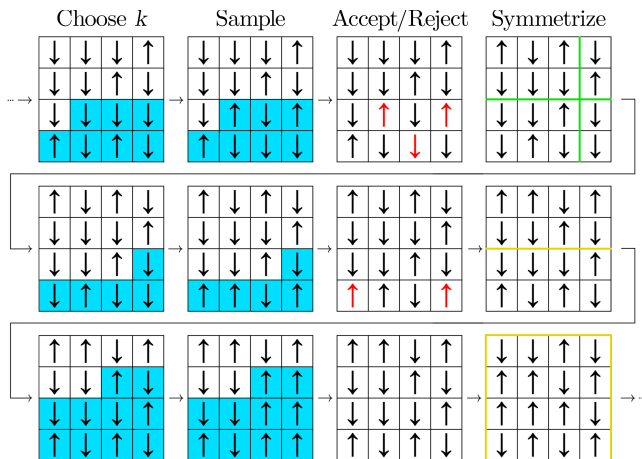


Figure 1. Example of three steps of NCUS applied to a  $4 \times 4$  spin model. The columns correspond to different lines in Alg. 1. The last  $k$  spins that can be flipped are highlighted in blue. If a proposal is accepted, the spins actually flipped are shown in red. For translations, the original borders of the lattice are shown in green. For reflections, the plane of reflection is shown in yellow, and yellow borders around the lattice indicate a reflection along  $z$ -axis (across  $xy$ -plane).

*Numerical experiments for the square-lattice Ising model.* We start to demonstrate the effectiveness of NCUS on the conventional two-dimensional Ising model:

$$E(\mathbf{s}) := \sum_{\langle ij \rangle} s_i s_j, \quad (3)$$

where  $\langle ij \rangle$  denotes a pair of nearest neighbors. The model can be solved exactly and has a critical point at  $\beta = \ln(1 + \sqrt{2})/2 \approx 0.44$  [37].

Our network architecture is based on PixelCNN [38], combined with dilated convolutions [39] to reduce the total number of parameters. Overall, our networks are lightweight and have 3 convolutional layers and approximately  $4 \times 10^3$  parameters. Thanks to the MCMC bias removal, we do not need the network to approximate the true distribution to an extremely high precision, which in any case will be increasingly difficult for larger lattices. As we use the same network for all the experiments, we can compare the performances of the various unbiased sampling methods. After training the network, we generate  $10^3$  Markov chains in parallel, each containing  $10^5$  samples [40].

When comparing the efficiencies of different MCMC algorithms, the main metric is the integrated autocorrelation time  $\tau$  [41], which determines the variance of the estimator when the variance of the observable and the sample size are given.  $\tau$  is an intrinsic property of the algorithm and the physical system, without dependence on the sample size, as long as we have enough samples to obtain a converged estimation of it. For NIS, the autocorrelation time is equal to one by definition; however, there is an increased variance arising from the reweighting pro-

cedure, which we consider as an effective autocorrelation time for sake of comparison with the other techniques.

From Fig. 2 (a), we see that both NGU and NIS have pathologically high autocorrelation times in the critical region. An inspection of their autocorrelation function [see Fig. 2 (b)] shows that the Markov chain of NGU is essentially non-ergodic in the available simulation time. By contrast, we see that our proposed method, NCUS, has no issue in the critical region. A closer inspection of the inset of Fig. 2 (a) shows that the autocorrelation time of NCUS still increases in the critical region, and the sampling efficiency is improved typically by 2 orders of magnitude compared with the global update methods. The performance of NCUS is comparable to the celebrated Wolff cluster update method, which is specifically designed for the Ising model [13]. Both NCUS and NGUS perform well in the critical region, and NCUS is to be preferred as the cluster update allows to achieve a lower autocorrelation time and, more importantly, a better asymptotic behavior of the autocorrelation function.

*Frustrated plaquette model.* We now study a model that presents a richer physics than the Ising model, and for which, to our knowledge, no traditional cluster update method is applicable. We consider a classical spin-1/2 system with nearest-neighbor  $J_1$ , next-next-nearest-neighbor  $J_3$ , and plaquette  $K$  interactions

$$E(\mathbf{s}) := J_1 \sum_{i,j=1}^L s_{i,j} (s_{i+1,j} + s_{i,j+1}) + J_3 \sum_{i,j=1}^L s_{i,j} (s_{i+2,j} + s_{i,j+2}) + K \sum_{i,j=1}^L s_{i,j} s_{i+1,j} s_{i,j+1} s_{i+1,j+1}, \quad (4)$$

which we denote as the frustrated plaquette model (FPM). In this work, we set  $J_1 = J_3 = -1$ .

We sketch the expected phase diagram in Fig. 3 (a) as a function of  $K > 0$ . The ground state of the FPM depend on the competition of  $J_1$  and  $K$ . For small  $K$  we expect a transition as a function of temperature between a paramagnetic (PM) and a ferromagnetic phase (FM), which is analogous to what found in the conventional Ising model. For  $K > 1$ , the ground state is a repetition of a  $2 \times 2$  unit cell containing one spin pointing in the opposite direction of the other three spins, as shown in Fig. 3 (a). The ground state breaks the  $\mathbb{Z}_2$  spin-inversion symmetry, and the  $\mathbb{Z}_2 \times \mathbb{Z}_2$  translation symmetry of one lattice spacing in  $x$  and  $y$  directions. As this phase has an average magnetization per site of  $1/2$ , we refer to this phase as ferrimagnetic (fM). At finite temperature, there must be a phase transition between the PM phase and the fM one, the nature of which we investigate in this work.

We present our numerical results for  $K = 2$  obtained

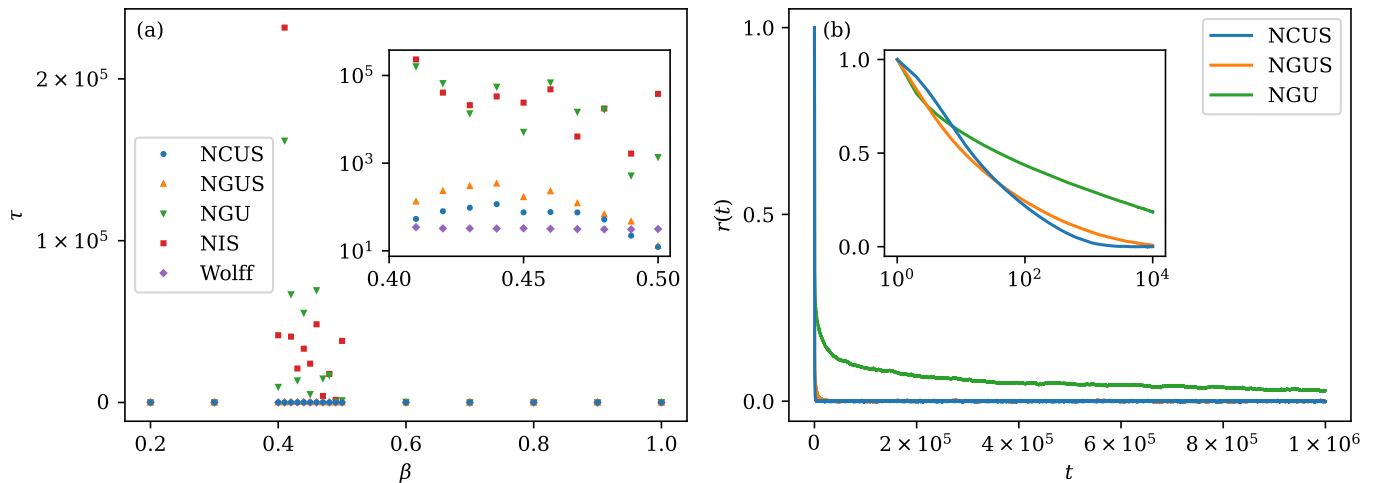


Figure 2. (a): Integrated autocorrelation time  $\tau$  as a function of temperature for the  $16 \times 16$  Ising model. For NIS, we use the increased variance from the reweighting procedure as the effective autocorrelation time. The inset focuses on their behaviors near the critical point, and uses logarithmic scale on  $y$ -axis. (b) Autocorrelation functions  $r(t)$  on  $16 \times 16$  Ising model at  $\beta = 0.44$ . The inset uses logarithmic scale on  $x$ -axis to focus on their behaviors at small  $t$ .

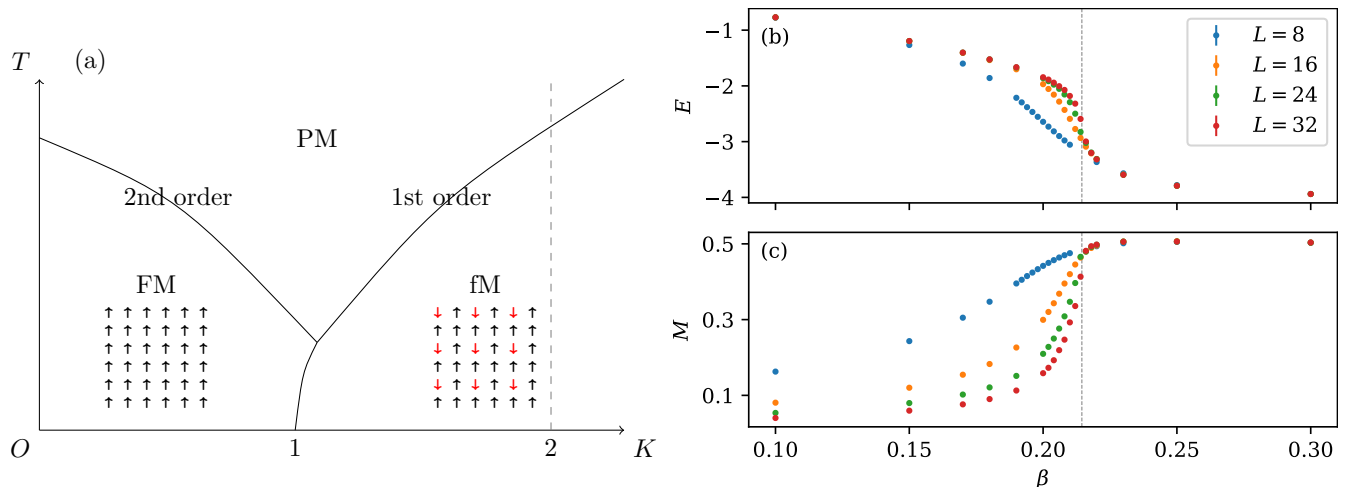


Figure 3. (a) Sketch of the expected phase diagram of the FPM for  $J_1 = J_3 = -1$  with example ground states in the ferromagnetic (FM) and the ferrimagnetic (fM) phases. The gray dashed line represents the temperature cut we numerically study. (b) Energy per site  $E$  and (c) spontaneous magnetization  $M$  per site of the FPM for  $J_1 = J_3 = -1$ ,  $K = 2$  as functions of temperature with lattice sizes up to  $L = 32$ , computed by NCUS. The gray dashed line indicates the estimated transition point  $\beta_c$ .

with NCUS for the average energy per site and the spontaneous magnetization per site  $M := \langle |\frac{1}{V} \sum_i s_i| \rangle$  in Fig. 3 (b, c) respectively, as functions of temperature with lattice sizes up to  $L = 32$ . Our data strongly suggest that in the thermodynamic limit  $L \rightarrow \infty$  the energy is discontinuous at the critical point  $\beta_c = 0.2145 \pm 0.0012$  with a latent heat  $Q = 1.36 \pm 0.20$ , estimated using the standard finite-size scaling procedure of Ref. [42]. Another indication of the first-order nature of the phase transition comes from the spontaneous magnetization shown in Fig. 3 (c), which, when extrapolated to the thermodynamic limit, shows a discontinuity of the spontaneous magnetization from 0 to a value close to  $1/2$ , as expected

for the fM phase [43].

Our results for the FPM show that the NCUS method is not affected by the metastability issues that are expected near first-order phase transitions [44–47]. As there are high free-energy barriers between different modes in the probability landscape that hinder the dynamics of local versions of MCMC, it is essential to have large clusters proposed directly from the neural network in order to rapidly explore the whole configuration space. Another potential issue for first-order phase transitions is the strong divergence of the specific heat, resulting in a high variance for the average energy. In spite of this, we are able to estimate the energy with high accuracy as

the error bars of Fig. 3 (b, c) are not visible.

*Conclusions.* In this Letter we have shown that it is possible to systematically remove the bias of variational autoregressive neural network methods by using them as cluster Monte Carlo update proposers. After having shown that global updates proposed from networks trained with the KL divergence are generically expected to fail because of a small number of exponentially suppressed configurations, we have provided a solution that takes advantage from enforcing the symmetries of the physical system and from using the chain-like graphical structure of the autoregressive model, in order to help the Markov chain rapidly escaping from ESCs. We have benchmarked our technique for the two-dimensional Ising model, showing in particular its efficacy in the critical region, where a straightforward implementation of neural global updates fails. We have further shown the potential of our method for systems for which no traditional cluster updates are known by considering a frustrated plaquette Ising model, where we were able to determine the first-order nature of a paramagnetic-ferrimagnetic phase transition breaking a  $\mathbb{Z}_2^3$  symmetry, remarking in particular that the automatic cluster updates we used allowed us to avoid metastability issues.

We acknowledge insightful comments and suggestions from Lei Wang and Pan Zhang. The computing power is supported with Cloud TPUs from Google's TensorFlow Research Cloud (TFRC). Our code is available at: <https://github.com/wdphy16/neural-cluster-update>

## Appendix A: Decomposition of transition matrix

The transition matrix  $M$  of a Markov chain is defined by

$$\boldsymbol{\pi}_{t+1} = M \boldsymbol{\pi}_t, \quad (\text{A1})$$

where  $\boldsymbol{\pi}_t$  is a state vector containing the probabilities of  $2^V$  configurations at sampling time  $t$ .  $M_{ij}$  is the probability to move from the configuration  $j$  to  $i$ .  $M$  has the *left stochastic property*

$$\sum_i M_{ij} = 1, \quad \forall j. \quad (\text{A2})$$

To improve the acceptance rate of the chain, we can write  $M$  as a convex combination of two transition matrices

$$M = \lambda M^{(1)} + (1 - \lambda) M^{(2)}, \quad (\text{A3})$$

or as a product of two transition matrices

$$M = M^{(2)} M^{(1)}, \quad (\text{A4})$$

where  $M^{(1)}$  and  $M^{(2)}$  are easier to sample than  $M$ . Given  $M^{(1)}$  and  $M^{(2)}$  are transition matrices,  $M$  must be a transition matrix and hold the left stochastic property.

In NCUS, we decompose  $M$  as

$$M = M_S M_K, \quad (\text{A5})$$

where  $M_S$  contains the symmetry operations, and  $M_K$  represents the cluster update. Specifically, we write  $M_K$  as convex combination of different-size cluster updates

$$M_K = \sum_{k=1}^V P_K(k) M^{(k)}, \quad (\text{A6})$$

where  $\sum_k P_K(k) = 1$ , and each of  $\{M^{(k)}\}$  contains the proposals and the rejections when only the last  $k$  spins are sampled.  $M^{(k)}$  with smaller  $k$  usually has higher acceptance rate. See Fig. 4 and Fig. 5 for a comparison of different choices of  $P_K$ . The sampling of  $M_S$  does not need rejection, because the symmetric configurations always have the same energy as the original one. We further decompose  $M_S$  as

$$M_S = M_{Rz} M_{Rd} M_{Ry} M_{Rx} M_{Ty} M_{Tx}, \quad (\text{A7})$$

where  $M_{Rx}$ ,  $M_{Ry}$ ,  $M_{Rd}$ , and  $M_{Rz}$  contain reflections along  $x$ -axis,  $y$ -axis, the diagonal, and  $z$ -axis respectively, and

$$M_{Tx} = \frac{1}{L} \sum_{i=0}^{L-1} M_{Tx;i}, \quad M_{Ty} = \frac{1}{L} \sum_{i=0}^{L-1} M_{Ty;i} \quad (\text{A8})$$

represent translations by  $i$  spins in the  $x$  and the  $y$  directions respectively. In this way, we naturally decompose the whole symmetry group into the direct product of subgroups, and avoid enumerating all the symmetry operations in sampling, while the number of symmetry operations can grow exponentially with the number of symmetry subgroups.

## Appendix B: Autocorrelation time

For Markov chain-based algorithms including NCUS, NGUS and NGU, we use the *integrated autocorrelation time* (IAT)  $\tau$  to characterize the efficiency of the algorithm [10]:

$$\tau = \sum_{t=1}^{t_{\text{cutoff}}} r(t), \quad r(t) = \frac{\tilde{r}(t)}{\tilde{r}(0)}, \quad (\text{B1})$$

with

$$\tilde{r}(t) = \left( \frac{1}{N-t} \sum_{i=1}^{N-t} O(\mathbf{s}^{(i)}) O(\mathbf{s}^{(i+t)}) \right) - \bar{O}^2, \quad (\text{B2})$$

where  $\{\mathbf{s}^{(1)}, \dots, \mathbf{s}^{(N)}\}$  are the samples in the Markov chain,  $O$  is the observable we are interested in, and  $\bar{O} = \frac{1}{N} \sum_{i=1}^N O(\mathbf{s}^{(i)})$ .

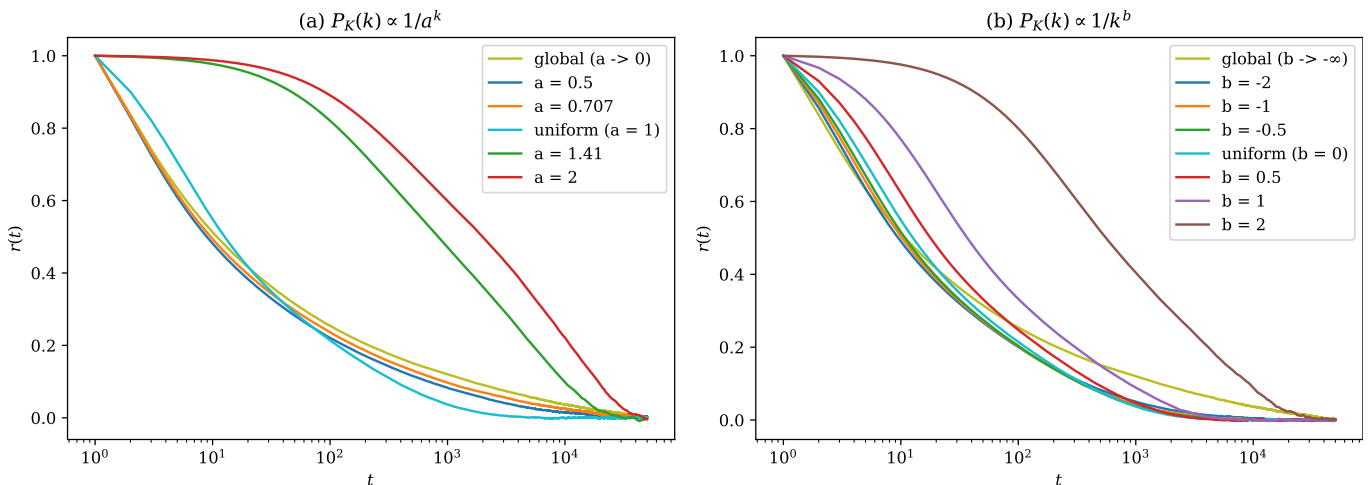


Figure 4. Autocorrelation functions  $r(t)$  by NCUS with various exponential and power distributions  $P_K$ , computed on  $16 \times 16$  Ising model. In general, the uniform distribution gives lower IAT than most other distributions we experimented.

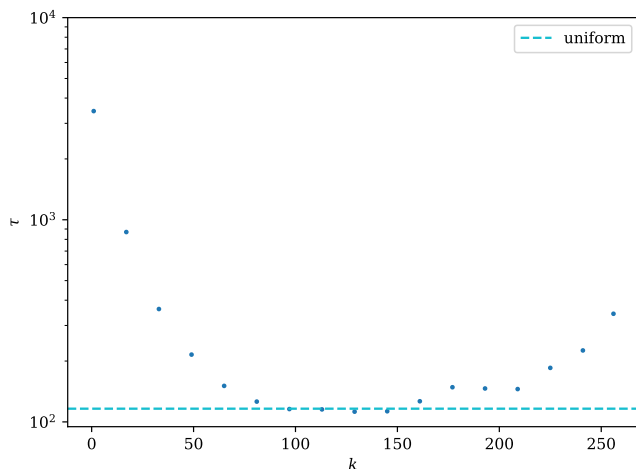


Figure 5. IATs when sampling with each  $k$  individually ( $P_K(k') = \delta(k' - k)$ ), computed on  $16 \times 16$  Ising model. The dashed horizontal line denotes the result with the uniform distribution. Although some medium-sized  $k$  give slightly lower IAT than the uniform distribution, it still performs better than most individual  $k$ .

Because the estimation of  $r(t)$  contains significant noise when  $t$  becomes large, we cut off  $t$  in the summation for  $\tau$  when  $r(t)$  crosses 0. The resulting IAT is insensitive to the cut-off point. If we change the threshold from 0 to 0.1, or cut off only when 100 consecutive  $r(t)$  are lower than the threshold, the relative change of  $\tau$  is  $< 10\%$ .

As we are drawing multiple Markov chains in parallel, we need an effective IAT to represent all of them. We first compute the variance  $\text{Var}[\bar{O}_i]$  of the observable estimator for each chain  $i$ :

$$\text{Var}[\bar{O}_i] = \frac{2\tau_i + 1}{n} \text{Var}[O_i], \quad (\text{B3})$$

where  $n$  is the chain length, and  $\text{Var}[O_i]$  is the variance of the data in this chain. Then we compute the expectation of the observable over all chains, and propagate the variance using the fact that the chains are independent of each other:

$$\text{Var}[\bar{O}] = \frac{1}{m} \sum_{i=1}^m \text{Var}[\bar{O}_i], \quad (\text{B4})$$

where  $m$  is the number of chains. Now the effective IAT  $\tau_{\text{eff}}$  can be solved from

$$\text{Var}[\bar{O}] = \frac{2\tau_{\text{eff}} + 1}{mn} \text{Var}[O], \quad (\text{B5})$$

where  $\text{Var}[O]$  is the variance of the data in all chains.  $\tau_{\text{eff}}$  is independent of the number of chains or the chain length, as long as we have enough samples to obtain a converged estimation.

We define an effective autocorrelation time for NIS by using the increased variance created by the reweighting procedure [48]

$$2\tau_{\text{eff}} + 1 = \frac{\text{Var}[wO]}{\text{Var}[O]} \quad (\text{B6})$$

### Appendix C: Details of numerical experiments

Our network has 3 convolutional layers, each with kernel size 5. The convolutions are masked to implement the autoregressive property, as introduced in PixelCNN [38]. The numbers of input, hidden, and output channels are  $1 \rightarrow 16 \rightarrow 16 \rightarrow 1$ . SiLU activations [49] are applied after the first and the second convolutional layers, which are reported to produce lower loss than ReLU. Sigmoid activation is applied after the third convolutional layer to restrain the output into  $(0, 1)$ . To be efficient in a

large number of sampling steps, we keep the network to be lightweight, while its receptive field should be able to approximately cover the whole lattice. So we use dilated convolutions [39] to expand the receptive field, and increase the dilation rate in each convolutional layer by a step size. The receptive field radius can be calculated by

$$\text{Receptive field radius} = \frac{1}{2}D((D-1)d+2)\frac{s-1}{2}, \quad (\text{C1})$$

where  $D = 3$  is the number of convolutional layers,  $s = 5$  is the convolution kernel size, and  $d$  is the dilation step size. For lattice sizes  $L = 8, 16, 24, 32$ , the dilation step sizes are 1, 2, 3, 4 respectively. The network has 3, 761 non-masked parameters in total, regardless of the lattice size.

During training, we use Adam optimizer [50] with conventional learning rate  $10^{-3}$ , batch size 64, and take  $2 \times 10^4$  training steps. To avoid being trapped in local minima, especially at low temperatures, in the first  $10^4$  steps we linearly anneal  $\beta$  from 0 to the desired value, which is reported to produce lower loss than exponential annealing. We do not use weight regularization or gradient clipping, because the network is shallow and there is no significant instability in training.

For sampling, we generate  $10^3$  Markov chains in parallel, each containing  $10^5$  samples. The chains are initialized by samples from the network. The first  $10^4$  samples in each chain are discarded, to make sure only the samples after thermalization are taken into account. For each experiment of NCUS up to  $L = 32$ , the Gelman–Rubin diagnostic [51] is  $< 1.1$ , which confirms the chains are thermalized. The IAT is  $< 4 \times 10^3$ , which is smaller than the remaining chain length by orders of magnitude.

---

\* dian.wu@epfl.ch

† riccardo.rossi@epfl.ch

‡ giuseppe.carleo@epfl.ch

- [1] N. Metropolis, A. W. Rosenbluth, M. N. Rosenbluth, A. H. Teller, and E. Teller, *J. Chem. Phys.* **21**, 1087 (1953).
- [2] K. Binder, *Monte Carlo and Molecular Dynamics Simulations in Polymer Science* (Oxford University Press, 1995).
- [3] K. Binder and D. W. Heermann, *Monte Carlo Simulation in Statistical Physics* (Springer Berlin Heidelberg, 2010).
- [4] W. Krauth, *Statistical Mechanics: Algorithms and Computations* (OUP Oxford, 2006).
- [5] J. Gubernatis, N. Kawashima, and P. Werner, *Quantum Monte Carlo Methods* (Cambridge University Press, 2016).
- [6] F. Becca and S. Sorella, *Quantum Monte Carlo Approaches for Correlated Systems* (Cambridge University Press, 2017).
- [7] S. Kirkpatrick, C. D. Gelatt, and M. P. Vecchi, *Science* **220**, 671 (1983).
- [8] R. Y. Rubinstein and D. P. Kroese, *The Cross-Entropy Method: A Unified Approach to Combinatorial Optimization, Monte-Carlo Simulation and Machine Learning* (Springer Science & Business Media, 2013).
- [9] R. L. Cook, *ACM Trans. Graph.* **5**, 51 (1986).
- [10] H. Müller-Krumbhaar and K. Binder, *J. Stat. Phys.* **8**, 1 (1973).
- [11] J. S. Liu, *Monte Carlo Strategies in Scientific Computing* (Springer Science & Business Media, 2008).
- [12] J.-S. Wang and R. H. Swendsen, *Physica A* **167**, 565 (1990).
- [13] U. Wolff, *Phys. Rev. Lett.* **62**, 361 (1989).
- [14] R. H. Swendsen and J.-S. Wang, *Phys. Rev. Lett.* **57**, 2607 (1986).
- [15] N. V. Prokof'ev, B. V. Svistunov, and I. S. Tupitsyn, *Phys. Lett. A* **238**, 253 (1998).
- [16] E. P. Bernard, W. Krauth, and D. B. Wilson, *Phys. Rev. E* **80**, 056704 (2009).
- [17] G. Carleo, I. Cirac, K. Cranmer, L. Daudet, M. Schuld, N. Tishby, L. Vogt-Maranto, and L. Zdeborová, *Rev. Mod. Phys.* **91**, 045002 (2019).
- [18] D. Levy, M. D. Hoffman, and J. Sohl-Dickstein, arXiv preprint arXiv:1711.09268 (2017).
- [19] J. Song, S. Zhao, and S. Ermon, arXiv preprint arXiv:1706.07561 (2017).
- [20] M. Medvidovic, J. Carrasquilla, L. E. Hayward, and B. Kulchytskyy, arXiv preprint arXiv:2012.01442 (2020).
- [21] J. Liu, Y. Qi, Z. Y. Meng, and L. Fu, *Phys. Rev. B* **95**, 041101 (2017).
- [22] L. Huang and L. Wang, *Phys. Rev. B* **95**, 035105 (2017).
- [23] H. Shen, J. Liu, and L. Fu, *Phys. Rev. B* **97**, 205140 (2018).
- [24] L. Bonati, Y.-Y. Zhang, and M. Parrinello, *Proc. Natl. Acad. Sci.* **116**, 17641 (2019), publisher: National Academy of Sciences; Section: Physical Sciences.
- [25] F. Noé, S. Olsson, J. Köhler, and H. Wu, *Science* **365**, 10.1126/science.aaw1147 (2019).
- [26] T. Müller, B. McWilliams, F. Rousselle, M. Gross, and J. Novák, *ACM Trans. Graph.* **38**, 1 (2019).
- [27] D. Wu, L. Wang, and P. Zhang, *Phys. Rev. Lett.* **122**, 080602 (2019).
- [28] M. S. Alberg, G. Kanwar, and P. E. Shanahan, *Phys. Rev. D* **100**, 034515 (2019).
- [29] S.-H. Li and L. Wang, *Phys. Rev. Lett.* **121**, 260601 (2018).
- [30] K. A. Nicoli, S. Nakajima, N. Strodthoff, W. Samek, K.-R. Müller, and P. Kessel, *Phys. Rev. E* **101**, 023304 (2020).
- [31] B. Uria, M.-A. Côté, K. Gregor, I. Murray, and H. Larochelle, *J. Mach. Learn. Res.* **17**, 7184 (2016).
- [32] H. Larochelle and I. Murray, in *Proceedings of the Fourteenth International Conference on Artificial Intelligence and Statistics*, Proceedings of Machine Learning Research, Vol. 15, edited by G. Gordon, D. Dunson, and M. Dudík (PMLR, Fort Lauderdale, FL, USA, 2011) pp. 29–37.
- [33] S. Kullback and R. A. Leibler, *Ann. Math. Stat.* **22**, 79 (1951).
- [34] In the context of variational inference, it was empirically found [52] that  $q$  tends to cover fewer modes than  $p$  in the probability landscape. However, the problem of exponentially suppressed configurations is more general as it is present even when all the modes are represented.
- [35] Formally, this is equivalent to multiply the Markov transition matrix by a matrix that leaves the equilibrium dis-

- tribution invariant, as discussed in the Supplemental Material.
- [36] A comparison of different choices of  $P_{\text{cluster}}$  can be found in the Supplemental Material.
- [37] L. Onsager, Phys. Rev. **65**, 117 (1944).
- [38] A. van den Oord, N. Kalchbrenner, and K. Kavukcuoglu, in *International Conference on Machine Learning* (PMLR, 2016).
- [39] F. Yu and V. Koltun, in *4th International Conference on Learning Representations, ICLR 2016, San Juan, Puerto Rico, May 2-4, 2016, Conference Track Proceedings*, edited by Y. Bengio and Y. LeCun (2016).
- [40] Details of the network structure, training and sampling are described in the Supplemental Material.
- [41] For completeness, we provide the definition of the autocorrelation function and the integrated autocorrelation time in the Supplemental Material.
- [42] K. Vollmayr, J. D. Reger, M. Scheucher, and K. Binder, Z. Phys., B Condens. Matter **91**, 113 (1993).
- [43] A naive Ginzburg–Landau approach for a three-component  $\mathbb{Z}_2 \times \mathbb{Z}_2 \times \mathbb{Z}_2$ -symmetric order parameter predicts a second-order transition when truncated at the quartic level. A first-order phase transition is also found in the  $q = 8$  Potts model [53–55], but the broken symmetry group there is  $\mathbb{Z}_8$ .
- [44] R. Gheissari and E. Lubetzky, arXiv preprint arXiv:1607.02182 (2016).
- [45] F. Krzakala and L. Zdeborová, Phys. Rev. Lett. **102**, 238701 (2009).
- [46] F. Krzakala, M. Mézard, F. Sausset, Y. F. Sun, and L. Zdeborová, Phys. Rev. X **2**, 021005 (2012).
- [47] J. Banks, R. Kleinberg, and C. Moore, arXiv preprint arXiv:1705.01194 (2017).
- [48] A. Kong, University of Chicago, Dept. of Statistics, Tech. Rep. **348** (1992).
- [49] S. Elfving, E. Uchibe, and K. Doya, Neural Netw. **107**, 3 (2018).
- [50] D. P. Kingma and J. Ba, in *International Conference on Machine Learning* (PMLR, 2015).
- [51] A. Gelman and D. B. Rubin, Stat. Sci. **7**, 457 (1992).
- [52] I. Goodfellow, Y. Bengio, and A. Courville, *Deep Learning* (MIT Press, 2016) Chap. 3.1.3.
- [53] H. Arisue and K. Tabata, in *Non-Perturbative Methods and Lattice QCD* (World Scientific, 2001) pp. 233–241.
- [54] V. Gorbenko, S. Rychkov, and B. Zan, J. High Energy Phys. **2018** (10), 1.
- [55] V. Gorbenko, S. Rychkov, and B. Zan, arXiv preprint arXiv:1808.04380 (2018).